Biosensors and Bioelectronics 153 (2020) 112054

Contents lists available at ScienceDirect

Biosensors and Bioelectronics

journal homepage: http://www.elsevier.com/locate/bios

Sensors design based on hybrid gold-silica nanostructures

Elnaz Bagheri [a,b,1], Legha Ansari [c,d,1], Elham Sameiyan [b], Khalil Abnous [a], Seyed Mohammad Taghdisi [e], Mohammad Ramezani [a,b,d,*], Mona Alibolandi [a,b,**]

[a] Pharmaceutical Research Center, Pharmaceutical Technology Institute, Mashhad University of Medical Sciences, Mashhad, Iran
[b] Department of Pharmaceutical Biotechnology, School of Pharmacy, Mashhad University of Medical Sciences, Mashhad, Iran
[c] Department of Pharmaceutical Nanotechnology, School of Pharmacy, Mashhad University of Medical Sciences, Mashhad, Iran
[d] Cellular and Molecular Research Center, Cellular and Molecular Medicine Institute, Urmia University of Medical Sciences , Urmia , Iran
[e] Targeted Drug Delivery Research Center, Pharmaceutical Technology Institute, Mashhad University of Medical Sciences, Mashhad, Iran

ARTICLE INFO

Keywords:
Hybrid
Silica
Gold nanoparticles
Sensor

ABSTRACT

Hybrid silica-gold based sensors show attractive performance in sensing technologies. Due to their interesting optical properties and biological compatibility, gold nanoparticles (AuNPs) have been extensively implemented in sensing technology.

Hybridization of AuNPs with silica NPs as a material with unique characteristic comprising large surface area, narrow pore distribution, tunable pore size and excellent charge transport provides great opportunity to fabricate promising sensing materials.

This review summarizes the current developments on sensing devices based on gold-silica hybrid materials and discussing their interest in designing biosensors for improved analytes detection.

1. Introduction

Among many types of nanoparticles in the field of biomedical and bioanalysis, silica is highly regarded because of its characteristics such as being nano-sized and mesoporous. Other features of silica nanoparticles include high surface-to-volume ratio, stability, large pore volume, controllable morphology and size, ease of preparation and biocompatibility (Chakraborty and Mascharak, 2016; Moreira et al., 2016; Song et al., 2017)

AuNPs based on molecular size divide into two subgroup consisted of few-nm AuNPs and few-atom Au nanoclusters. AuNPs are known as nanoclusters (NCs) (0.8 up to 15 nm), when the size scale is extremely small (Zhang et al., 2012a,b).

AuNPs with controlled sizes and shapes have electromagnetic, catalytic, electrochemical and plasmonic properties introducing them as an important element in sensors design (Taei et al., 2015). However, AuNPs with sizes below 200 nm may form aggregates which are stable with high surface energy thereby making them unsuitable for long-term application. Thus, porous supports such as SiO_2 was used for anchoring AuNPs to overcome this problem. The fundamental advantages such as high surface to volume ratio of nanomaterials make them naturally reactive materials. Thus they are suitable as sensor and catalyst materials. Silica as support material was used for Au nanocatalyst design and other catalytic applications such as catalytic activity enhancers *via* either synergetic effects of the silica support, or preventing AuNPs from aggregation (Bracamonte et al., 2017; Ji et al., 2011; Liu et al., 2014). AuNPs-decorated SiO_2 microspheres improve catalytic activity of AuNPs, salt stability, and versatile surface functionalization (Wang et al., 2013a). Furthermore, AuNPs could be used as capping agent inhibiting leaking out of cargo from mesoporous silica nanoparticles (MSN) and could be uncapped under controlled conditions to release the payload.

There are several methods for the preparation of silica/Au nanoclusters such as organizing Au nanoclusters on the silica precursor or silica support in the presence of a thiolate ligand or a protein (i.e. BSA) (Lavenn et al., 2012, 2014; Wang et al., 2013b), deposition of AuNPs on silica beads by reducing Au^{3+} ions using citrate (Sousa-Castillo et al., 2015), and fabrication of Au clusters by ion beam mixing using irradiation on Au/SiO_2 followed by annealing at high temperature (Dhara et al., 2004).

* Corresponding author. Nanotechnology Research Center, School of Pharmacy, Mashhad University of Medical Sciences, Mashhad, Iran.
** Corresponding author. Pharmaceutical Research Center, School of Pharmacy, Mashhad University of Medical Sciences, Mashhad, Iran.
E-mail addresses: ramezanim@mums.ac.ir (M. Ramezani), alibolandim@mums.ac.ir (M. Alibolandi).
[1] These two authors contributed equally to this work.

https://doi.org/10.1016/j.bios.2020.112054
Received 25 May 2019; Received in revised form 11 January 2020; Accepted 25 January 2020
Available online 28 January 2020

An ideal sensor should have features such as robustness, precision, accuracy, selectivity, sensitivity, linearity and reproducibility. AuNPs present in silica-gold hybrid systems exhibit particular features and easy synthesis making it suitable for fabrication of electrochemical, fluorescence, colorimetric, surface-enhanced Raman spectroscopy (SERS) and optical sensors for analytes detection. Thus silica/Au hybrids could be employed for the design of a wide range of sensors summarized in Table 1.

2. Gold

Gold conjugates with mesoporous silica nanoparticles have high compatibility properties with medical applications and unique mesoporous structure. The advantage of porous silica coating is to provide an effective pathway for reactant molecules to reach the surface of AuNPs. The porous structures provide an efficient pathway for reactant molecules to access the surface of Au electrodes.

High specific surface of gold nanostructures is an appropriate option for loading various targets to construct multifunctional nanocarriers (Zhu et al., 2015). In particular, AuNPs are an ideal material to prepare chemical sensors, bio-imaging agents and bio-medicine due to their suitable size, non-toxic, simple preparation methods, unique optical and electronic properties. These gold nanoparticles composite (AuNCs) have quantum confinement, two-photon absorption, high quantum yields (QYs) and red-emission properties (Chand and Neethirajan 2017). However, only few studies have investigated gold-based hybrid nanomaterials for realtime and *in vivo* biosensing in clinical applications. Copper nanoclusters (CuNCs) are cheaper than AuNCs and AgNCs. However, CuNCs would be oxidized easily and their fluorescence would be quenched, thereby limiting the use of CuNCs as an alternative to AuNCs and AgNCs (Chand and Neethirajan 2017).

2.1. Fluorescence sensor

In fluorescent systems, the fluorescent molecules are encapsulated within the pores leading to the quenched fluorescence signal. Among different signal transduction sensors, fluorescent sensors have unique properties such as easy setup, suitable signal transduction, wide linear range and quick response. Plasmonic excitations in metallic nanocomposite increase molecular fluorescence intensities (Li et al., 2016). Thus, SiO_2_AuNPs conjugation, provides biocompatibility, versatile surface functionalization and good hydrophilicity (Yang et al., 2018).

Furthermore, fluorescence-based sensors provide sensitive sensing platform because of the availability of various methods for determining

Table 1
Representation of silica-AuNPs hybrid sensors.

Detection approach	Nanoparticle	Role of the silica and AuNPs	Detection sample	LOD (CFU/mL)	Ref.
fluorescence sensor	Au NBP@SiO_2@Cy_7	Silica as the cover, Au NBP as core	pyrophosphate and Cu^{2+}	–	Niu et al. (2016)
fluorescence sensor	Fe_3O_4@SiO_2–AuNCs	Fe_3O_4@SiO_2as cover BSA-capped Au nanoclusters as core	6-mercaptopurine	–	Li et al. (2015b)
fluorescence biosensor	MNCPs	Fe_3O_4 as core coated with SiO_2 and Au loaded on the surface of SiO_2	PSA	3.0- × 10^{-13} g/mL	Yang et al. (2018)
SERS	Fe_3O_4@SiO_2@Au@Ag	Fe_3O_4@SiO_2 as core Au@Ag as shell	p-ATP and thiram	5 × 10^{-14} M and 5 × 10^{-11} M	Sun et al. (2018b)
SERS	microfluidic chip	Packed silica microbeads isolated solid or larger sized particles and The Grp-AuNPs composite	norovirus	100 pM	Chand and Neethirajan (2017)
SERS	SEHGNs magnetic beads	Hollow gold nanoparticles as core silica as shell- anti-ATB1 antibody-conjugate magnetic beads	aflatoxin B1	–	Ko et al. (2015)
SERS	SA@GNP and Au@MNP	Silica coated AuNP as core And gold-coated paramagnetic nanoparticles	miRNA-141	1.8 pM	Zhang et al. (2018)
SERS	AuNPs covered on SiO_2 nanospheres	AuNPs as shell and SiO_2 as core	TBZ. CV. 4-ATP	10^{-6}M to 10^{-18}M	Phatangare et al. (2018)
SERS	SiO_2@Au core/shell @DNA aptamer	SiO_2 as core and AuNP as shell	Hg^{2+}	10 nM	Lu et al. (2018b)
SERS	SEGNs and magnetic nanoparticles (MNPs) as capture probe	Silica as shell AuNPs as core And magnetic nanoparticles (MNPs) as capture probe	*E. coli* O157:H7	10 CFU mL^{-1}	Zhu et al. (2018)
electrochemiluminescence (ECL) biosensor	$F_{e3}O_4$@SiO_2@AuNPs-CP Ru $(phen)_3^{2+}$ HCR/GO	$F_{e3}O_4$ as core and SiO_2 coated the surface of Fe_3O_4 and Au covered them.	miRNA-141	–	Lu et al. (2018a)
electrochemiluminescence aptasensor	RuSiNPs@PLL-Au Au NPs on 3D graphene-modified electrode	SiNPs as core and Au as shell	lysozyme	7.5 × 10^{-13} mol L^{-1}	Du et al. (2018)
electrochemical aptasensor	AuNPs/amine-functionalized silica nanoparticle	Fe_3O_4 as core and the d silica as the shell AuNPs were immobilized on the Fe3O4@SiO2 surface	Tryptophan	0.026 nM	Hashkavayi and Raoof (2017)
electrochemical biosensors	AuNPs-GO modified GCE SiO_2@Ag/DNA	SiO_2 as core and Ag as shell gold nanoparticles-reduced graphene oxide (AuNPs-GO) altered glass carbon electrode (GCE)	BRCA-1	2.53 fM	You et al. (2018)
electrochemiluminescence (ECL) immunosensor	Cu/Ni/Ru and Au@PEI@SiO_2	SiO_2 as core and Au as shell	aflatoxins B1	0.0039 ng mL^{-1}	Wang et al. (2018)
electrochemical aptasensor	Mesoporous silica thin films (MSF) Au electrode	MSF on the Au electrode	PSA	280 pg mL^{-1}	Argoubi et al. (2018)
electrochemical aptasensor	Fe3O4@Ag/mSiO2/AuNPs	$mSiO_2$ as core and AuNPs as shell	CRP	0.0017 ng mL^{-1}	Wang et al. (2017)
Colorimetric sensor	Fe_3O_4@SiO_2@AuMNPs	Fe_3O_4 as core, sio_2 as shell and AuNPs functionalized SiO_2	glucose	3 mM	Luo et al. (2017)
Colorimetric sensor	gold nanorod@silver@SiO_2	AuNR@Ag as core and Mesoporous silica as shell	AA	0.03 Mm	Chen et al. (2019)

the absorbance and fluorescence. This advantage is due to measurement of the fluorescence relative to a dark background, as compared to the bright reference beam in an absorbance measurement. It is easy to detect low levels of light, and the electronic impulses due to single photons are measurable with most photomultiplier devices. However, short lifetime of some fluorescent dyes poses an important limitation, which could be overcome by implementing long-lifetime metal ligand probes comprising ruthenium, osmium, or rhenium.

In the work by Niu and coworkers, a novel near-infrared (NIR) plasmon-enhanced fluorescence (PEF) probe consisting of elongated gold nanobipyramids antennas, silica, and NIR dyes (Au NBP@Si-O_2@Cy7) was fabricated (Silica as shell, Au NBP as core). This biosensor not only could detect pyrophosphate and Cu^{2+} in living cells but also could be used for a microRNA assay (Niu et al., 2016). However, fluorescent labeling, bulky sensing instrumentation, the high cost of application and preparation of specific metal nanoclusters have limited their utilization for fabrication of fluorescence sensor (Niu et al., 2016).

In another study, a novel non-toxic sensor has been prepared as Fe_3O_4@SiO_2, surrounded with BSA-capped Au nano-clusters (AuNCs) for 6-mercaptopurine (6-MP) detection (Fe_3O_4@SiO_2 as cover, BSA-capped Au nano-clusters as core). 6-MP is prescribed for the treatment of cancer and autoimmune diseases by inhibiting the synthesis of purine. Due to the serious side effects associated with this drug, the blood concentration of the 6-MP must be controlled in the patient during administration. In the prepared system, even in the presence of oxidants, phenols, heavy-metal ions, and especially bio-thiols, 6-MP can selectively quench the fluorescence of Fe_3O_4@SiO_2–AuNCs due to AuNCs aggregation, and facilitation of the destruction of the cross-linked Fe_3O_4 @SiO_2 and AuNCs structure. Thus, in the presence of 6-MP, cross-linkers within AuNC structure and the Fe_3O_4 NPs@SiO_2 were cleaved, leading to a red fluorescence emission. As a result, Fe_3O_4@SiO_2–AuNCs acted as fluorescence sensor (Li et al., 2015b). Given that prostate cancer is one of the most common malignancies in man (Fuerea et al., 2016), early diagnosis of prostate-specific antigen (PSA) could help in the early identification of prostate cancer (Wang et al., 2015). In this regard, an oligopeptide (HSSKLQ, a substrate for PSA enzyme) based fluorescence biosensor was developed in order to provide rapid and simple detection of PSA. Due to the high sensitivity and selectivity of the peptide, the prepared peptide/Fe_3O_4@SiO_2–Au nanostructures (MNCPs) (Fe_3O_4 as core coated with SiO_2 and Au loaded on the surface of SiO_2), might be an ideal platform for monitoring the enzyme activity of PSA with high specificity. The role of SiO_2 in MNCPs is to improve salt stability of AuNPs. Fe_3O_4 and gold segments (AuNPs) were used for rapid magnetic separation and fluorescence quenching of FAM-peptides conjugate, respectively. This biosensor was based on self-assemble 5-FAM labeled peptides onto the surface of MNCPs, led to efficient quenching. In the presence of PSA, PSA cleaved the FAM-peptides and consequently the MNCPs surface emitted fluorescence. Thus, fluorescence recovery occurred. The limit of detection of this fluorescent biosensor for PSA biomarker was 3.0- $\times 10^{-13}$ g/mL. Due to the low LOD, this biosensor platform has the great potential for implementation in biological and clinical analysis (Yang et al., 2018). Nevertheless, the use of enzyme-functionalized nanomaterials is limited because of denaturation and leakage of enzymes as well as costly purification and preparation methods involved.

More examples of fluorescent sensors based on silica-Au hybrid NPs are summarized in Table 2.

Table 2
Fluorescent sensor based on silica-gold hybrid NPs.

Detection approach	Nanoparticle	Detection sample	LOD (CFU/mL)	Ref.
Fluorescent aptamer-based sensor	SNPs-AuNPs-streptavidin	Cocaine	209 pM	Emrani et al. (2016)
FRET-based sensors	AuNP@SiO_2MSN	ATP	0.1 nM	Li et al. (2016)
Fluorescent sensor	BSA- Au nano-clusters capped core-shell Fe_3O_4–SiO_2 nanoparticles	6-Mercaptopurine (6-MP)	0.004 μmol L^{-1}	Li et al. (2015b)
Fluorescent sensor	NRs@SiO_2-AO (Acridine orange-loaded mesoporous silica-coated gold nanorods)	BSA and ctDNA (calf thymus DNA)	0.25 mol/L. 0.1667 μg/mL	Zhu et al. (2015)

2.2. SERS biosensor

Surface-enhanced Raman scattering (SERS) with unique spectroscopic fingerprint and high sensitivity properties detects small bioactive molecules such as DNA and proteins. Considering that the absorption peaks of silver and gold nanostructures are in near–infrared and visible regions, Au and Ag nanostructures are significantly effective in amplifying SERS enhancement, because the surface plasmon range of Au and Ag improves SERS effect (Li et al., 2015a). Modifying thickness ratio of core and shell can control the optical properties of the nanocomposite (Liu et al., 2011). In this regard, Au shells on the surface of paramagnetic nanoparticles (MNPs) core could form SERS-active junction regions (hot spots) and thereby enhancing the intensity of SERS signaling (Zhang et al., 2018).

While SERS remains one of the most powerful analytical techniques available, advances in SERS capabilities often lie in the substrates used. Silica-gold hybrid platform represents advantage of well-controlled and strongly-coupled particles or films for obtaining maximum enhancement. On the other hand, SERS substrate development with silica-gold hybrid may open up near UV and UV regions of the spectrum to SERS.

Since the surface ligands, particle size and valence states have influence on the luminescent AuNPs properties and play a key role in the emission, AuNPs based on the luminescent properties were divided into TREE groups: plasmonic NPs, few-nm NPs and nanoclusters. Au nanoclusters (AuNCs) like other gold nanosystems have optical and electrochemical properties. ECL signal from AuNP@SiO_2 electrode was observed 5 times higher than that of the SiO_2 nanoparticles.

Aflatoxin B1 (AFB1) is a hazardous carcinogenic compound, found in spoiled foods (Manso et al., 2014). SERS is an important optical technique which has been utilized for analyte sensing and SERS imaging. In this regard, Ko et al. designed a SERS-based immunoassay technique for aflatoxin B1 (AFB1) detection using magnetic beads and silica-encapsulated hollow gold NPs (SEHGNs). It should be noted that AFB1 has two different types of binding epitopes. Thus in the prepared platform, two different antibodies against AFB1 were implemented in order to form an immunocomplex. In this regard, anti-AFB1s and anti-ATB1 were conjugated onto the surfaces of SEHGNs and magnetic beads, respectively helping the formation of an immunocomplex sandwich in the presence of target molecule AFB1. In this system, HGNs operated for measureable analysis of AFB1 as reproducible sensing probes, silica coating prohibited adsorption of external species and desorption of Raman reporter molecules and magnetic beads were applied as supporting substrates for highly sensitive recognition of AFB1. The aforementioned platform was developed as highly stable SERS-encoding based immunoassay. The rapid, selective and reproducible quantitative analysis of AFB1 was performed by monitoring the intensity change of the characteristic peaks of Raman reporter molecules. The attachment of metallic nanoparticles to supporting substrates is advantageous due to the increase in the effective surface volume ratio of these nanoparticles. As a result, SEHGNs were applied as analytical platform while magnetic beads acted as sensitive detection parts (Ko et al., 2015). There are various SERS biosensors for the recognition of foodborne microorganisms. However, complex system, bulky instrumentation, limited quantification capability are some disadvantages of

this method.

One of the general causes of gastroenteritis outbreaks in the world are noroviruses. Due to the resistance of these viruses to thermal and general disinfectants, rapid detection in clinical and food samples is extremely essential. An all-polydimethylsiloxane microfluidic chip merged with silica microbeads was applied as microfiltration zone for isolation large or solid particles from the solution. Graphene-gold nanocomposite was employed for a ferrocene-tagged aptamer immobilization and one-step electrochemical detection of norovirus. When norovirus interacted with a ferrocene-tagged aptamer, the electrochemical signal from ferrocene was reduced. This microfluidic chip was applied to quantify the norovirus with a limit of detection of 100 pM (Chand and Neethirajan 2017). It is should be noted that the aptamer-based sensors compared to antibody-based ones benefit from remarkable advantages, such as high reproducibility, high thermal resistance, small size, good biocompatibility, low cost, and facile production and modification.

Sun and coworkers applied a new SERS nanocarrier for p-ATP and thiram (pesticide) detection. This nanocomposite was composed of a 600 nm Fe_3O_4 core covered by a 10 nm silica shell with superparamagnetic properties and cube shape. In order to maintain magnetic property of Fe_3O_4@SiO_2 and preventing aggregation, the cationic PEI was used to coat Fe_3O_4@SiO_2 core. The NH_2 groups of PEI provided appropriate surface functionality for strong metal interaction. The Au@Ag particles accumulated on the surface of Fe_3O_4@SiO_2 core form the Fe_3O_4@SiO_2@Au@Ag complex using the interaction between Ag and NH_2 groups of PEI (Fe_3O_4@SiO_2 as core, Au@Ag as shell). The Au@Ag showed plasmonic property and potential SERS activity. Hybrid metals (Ag, Au) nanocomposites with target molecules (p-ATP and thiram) bound *via* S–S bond formation causing SERS amplification. The limit of detection of this biosensor for p-ATP and thiram was 5×10^{-14} M and 5×10^{-11} M, respectively (Sun et al., 2018b). This system with high SERS activity applied for the detection of biological, chemical and environment pollutants at trace level.

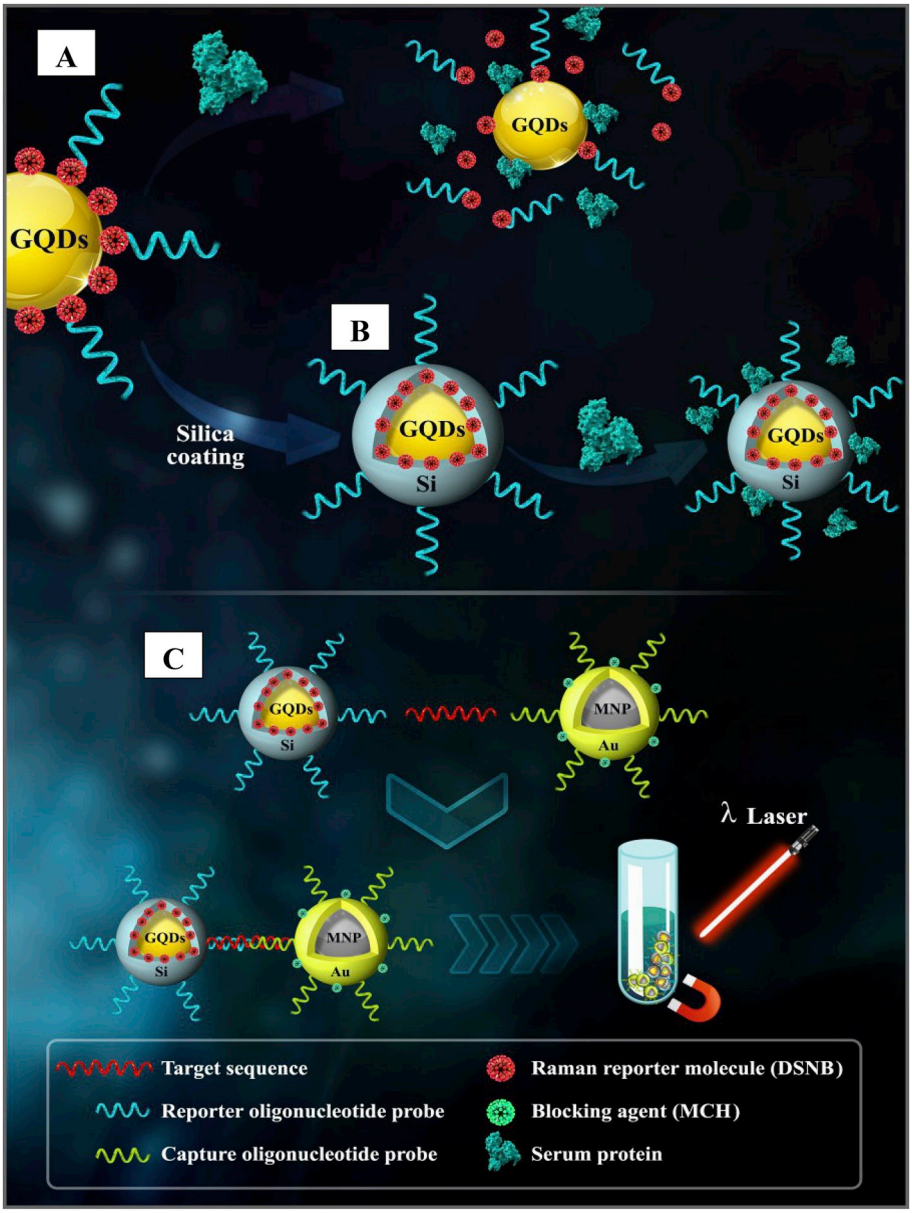

Fig. 1. Schematic representation of A) in the absence of silica coating, Raman reporter molecules was replaced with serum protein. B) SA@GNPs nanostructure preventing protein adsorption. C) SA@GNPs as capture probe and SERS recognition of target miRNA-141 beside Au@MNPs conjugated with capture probes acted as magnetic substrates. Reproduced with modification from (Zhang et al., 2018).

In another study, Zhang and coworkers designed magnetic-based SERS system for cancer-related miRNA-141 detection. This system is made of two capture nanostructures with high sensitivity and reproducibility. A glass shell of silica-covered AuNPs with a thickness of 13 nm was functionalized with Raman-active molecules, 5,5′-dithiobis (succinimidyl-2-nitrobenzoate) (DSNB). Reporter probes conjugated on the surface of silica shell acted as SERS nanotag. Another part of sandwich structure was gold-coated paramagnetic nanoparticles (Au@MNPs). This part was conjugated with capture probes and acted as magnetic substrates. The miRNA-141 oligonucleotide was hybridized with both oligonucleotide and capture probes to form the SA@GNP/miRNA-141/Au@MNP complex. An external magnet isolated the SA@GNP/miRNA-141/Au@MNP complex from the solution and laser excitation of the DSNB-GNPs provided a SERS signature spectrum diagnostic of the analyte molecules (Fig. 1). The limit of detection (LOD) of this system for miRNA-141 sequences in serum was 1.8 pM (Zhang et al., 2018). This biosensor confirmed the important role of silica coating in preventing the dissociation of Raman reporters from the GNPs and used for reproducible and quantitative detection of serum miRNAs.

In another study, Phatangare and coworkers applied nanosensors for pesticides and dyes detection. In this system, 3 nm AuNPs covered on SiO_2 nanospheres (of size ~ 240 nm) were made by the electron irradiation process with 6 MeV (AuNPs as shell and SiO_2 as core). Actually, the connection between two metal surfaces or nanoscale gap between two metal nanospheres was termed hot spot. A very high electric field was generated by the laser excitation in appropriate wavelength. During the SERS studies using this system, the strong electric field in the hotspots can be produced by the incident laser radiation and used as reporter molecules. They used these nanoparticles for fingerprint detection of thiabendazole (TBZ), crystal violet (CV) and 4-aminothiophenol (4-ATP). Au nanospheres as the SERS substrates could detect pesticides and dyes at an ultra-low concentration (10^{-6}M to 10^{-18}M) using 785 nm laser radiation (Phatangare et al., 2018).

Mercury (II) (Hg^{2+}) especially methyl mercury causes serious disease and damages to organs of the human body such as central nervous system, kidney and digestive system (Clarkson et al., 2003). Lu and coworkers applied label-free SERS sensor for Hg^{2+} detection in aqueous solution. This sensor is consisted of SiO_2@Au core/shell nanoparticles (NPs) coated with DNA aptamer (SiO_2 as core and AuNP as shell). DNA aptamer comprises of two parts; one part of aptamer was consisted of consecutive thymines (T) served as capture part which interacts with Hg^{2+} and the other part included adenine (A) and guanine (G) as the Raman signal reporters. In the presence of Hg^{2+}, it interacted with single-stranded DNA (T-Hg^{2+}-T pairs) contained thymines generating vertical orientation of DNA molecule. Raman intensity of A and G bases in the DNA strands was enhanced with increase of Hg^{2+} concentration. This biosensor could detect Hg^{2+} concentration as low as 10 nM (Lu et al., 2018b).

In another study, a stable SERS tag of silica shell coated AuNPs (SEGNs) as signal probe and magnetic nanoparticles (MNPs) as capture probe for separation (Silica as shell, AuNPs as core and magnetic nanoparticles (MNPs) as capture probe) were utilized for *Escherichia coli* O157:H7 (*E. coli* O157:H7) detection. In this system, 4,4′- dipyridyl (DP) was used as Raman reporter embedded between silica shell and AuNPs core. The thick silica shell prevented the DP leakage from the surface of AuNPs thereby inhibiting the interaction between possible impurities and DP as the Raman reporter. The signal of the SERS active site greatly increased. Capture and signal probes, which were conjugated with a pair of antibodies, were used separately for the sensitive and specific separation of *E. coli* O157:H7. One antibody was conjugated with the capture probe and the other antibody was immobilized on the surface of signal probe. Subsequently, in the presence of *E. coli* O157:H7, sandwich structure of antibody-antigen-antibody was formed and separated with the help of magnet. By increasing the number of *E. coli* O157:H7, signal probes related to the Raman signal intensities would decrease. The limit of detection of this sensor was as low as 10 CFU mL^{-1} (Zhu et al., 2018). Other SERS sensors were summarized in Table 3.

2.3. Electrochemical (ECL) biosensor

Electrochemical biosensors with simple instrumentation, intrinsic, sensitive, selective and rapid properties are suitable biosensor for several bio-analyte detections including metabolic markers, viruses, enzymes, etc.

In this system, numerous bio-recognition receptors such as aptamer, antibodies, etc. were applied as detector immobilizer on the surface of electrode (Chand and Neethirajan 2017). The electrode of the electrochemical (ECL) biosensors could flow the electrons freely to the signal unit. Many materials such as conjugated polymers (Gaylord et al., 2005). Enzymes (Liu et al., 2015), and hybrid nanoparticles are used in electrochemical sensors for signal production (Bagheri et al., 2018). Nanostructured silica as support material guide electro-catalytic activity of the metal NPs immobilized on their surface (Sápi et al., 2017; Shim et al., 2012). AuNPs with electrochemical, plasmonic, catalytic properties and controlled sizes and shapes have a major potential in many reactions (Taei et al., 2015). Moreover, the conductivity of the produced sensor could be improved due to AuNPs. Electrical biosensors have higher sensitivity compared to fluorescence and colorimetric immunoassays. However, the condition of their recognition environment such as ionic strength and solution pH can alter the sensing results.

Electrochemical sensors provide some advantages including good resolution, low power requirements, accuracy and excellent repeatability. However, short shelf life, high temperature sensitivity and environmental diversity and sometimes cross-sensitivity to other identical analytes limit its high sensitivity toward its target.

miRNA is an important biomarker for molecular diagnosis of cancer cell. Since, the concentration of the miRNAs in cancer cells is low, high-sensitivity method for biomarker detection is essential (Cissell et al., 2007). In this regard, Lu et al. applied an electrochemiluminescence (ECL) biosensor for femtomolar miRNA-141 detection. One of the common modes of the ECL biosensor is sandwich-type with low cost and high sensitivity properties. The biosensor is composed of two parts: signal unit (Ru (phen)$_3^{2+}$ HCR/GO) (Tris (bipyridine)ruthenium (II) hybridization chain/graphene oxide) and capture unit (Fe_3O_4@-SiO_2@AuNPs) (Fe_3O_4 as core and SiO_2 immobilized on the surface of Fe_3O_4 and Au as shell). Firstly, trigger probe (TP) interacted with GO *via* covalent bonding of amino-carboxyl and then two hairpins DNA of H1 and H2 were presented to TP/GO solution. In the presence of TP, H1 and H2 were hybridized. Finally, Ru (phen)$_3^{2+}$ molecules interacted with the dsDNA polymers and Ru (phen)$_3^{2+}$ HCR/GO complex was formed. By increasing hybridization of the DNA skeleton, absorption of Ru (phen)$_3^{2+}$ and electrochemiluminophores were improved. On the other hand, in the presence of target miRNA-141, stem-loop structure of capture probe (CP) which was immobilized on Fe_3O_4@SiO_2@AuNPs was opened and interacted with target miRNA-141. In addition, the end residues

Table 3
Representation of SERS-based sensors.

Detection method	Nanoparticle	Detected sample	LOD (CFU/mL)	Ref
SERS	Au@AgNP@SiO2@Nc-Van	Vancomycin (Van)-resistant enterococci	–	Zhou et al. (2018)
SERS	AuNPs@mesoSiO$_2$	Diluted blood trace	–	Zou et al. (2017)
SERS	Fe_3O_4@Ag/mSiO$_2$/AuNPs	Methotrexate	1 nM	Chen et al. (2017)
SERS	SiO$_2$@Au	Cd^{2+}	2 ppm	Thatai et al. (2015)

sequence of CP was hybridized with H2 and formed a Faraday cage-type structure (Fig. 2) leading to the emission of ECL signal. Higher concentration of miRNA-141 led to the combination of more Ru $(phen)_3^{2+}$ thereby increasing ECL signal intensities (Lu et al., 2018a).

Application of ECL luminophore is limited due to poor water solubility and low aqueous stability of the electrochemical reactions.

Lysozyme is an antimicrobial enzyme, which can hydrolyze glycosidic bonds between N-acetylglucosamine and N-acetylmuramic acid exist in peptidoglycan residues of gram-positive bacterial cell walls (Smith et al., 1973). Due to the dependence of lysine levels on malignant diseases such as cancer, myeloid leukemia and HIV, Du et al. designed electrochemiluminescence (ECL) based techniques with high sensitivity, stability, and low detection limit for lysozyme isolation. Tris (2, 2′-bipyridyl) ruthenium (II) $(Ru(bpy)_3^{2+})$ has been pursued as chemiluminescent reagent and anchored on an electrode surface. Two parts of the electrochemiluminescence aptasensor were composed of Ru $(bpy)_3^{2+}$-Silica@Poly-L-lysine-Au (RuSiNPs@PLL-Au) nanocomposites as an indicator and AuNPs on 3D graphene-modified electrode as substrate electrode (SiNPs as core and Au as shell). The lysozyme binding aptamer (LBA) through gold-thiol interaction was hybridized with the 3D graphene/AuNPs electrode and attached to the complementary single-strand DNA (CDNA) of the lysozyme aptamer, which was coated on RuSiNPs@PLL-Au as an electrochemiluminescence intensity amplifier. Because of this interaction, the ECL intensity of the aptasensor increased. In the presence of lysozyme, the lysozyme replaced the CDNA segment of the self-assembled duplex leading to the reduction of the electrochemiluminescence signal. The detection limit of this biosensor was estimated to be 7.5×10^{-13} mol L^{-1} (Du et al., 2018).

Tryptophan (Trp) is an essential amino acid for the production of melatonin (Knott and Curzon, 1972), serotonin, and niacin in human body (Ya et al., 2008). Because our body cannot make Trp, it must be added to the consumable food. One of the diagnostic methods for diseases such as liver cancer, colorectal cancer, autism and depression is to estimate the concentration of free Trp in blood plasma in these patients (Capuron et al., 2002). Since the concentration of tryptophan in blood plasma is low, Hashkavayi et al. designed a selective and sensitive electrochemical aptasensor for quantification of Trp. The immobilization of aptamer for detection of tryptophan on the surface of the AuNPs/amine-functionalized silica nanoparticle was monitored by hemin (Hem) operating as electrochemical biosensor (Fe_3O_4 as core and silica as the shell formed Fe_3O_4@SiO_2 structure, then AuNPs were electrodeposited on the Fe_3O_4@SiO_2 surface). Hem, interacted with guanine bases of the aptamer, and acted as a redox scale to produce a readable electrochemical signal by changing the aptamer conformation. In the presence of Trp, the conformation of aptamer reformed and Trp approached the electrode surface. Thus, voltammetry and electrochemical impedance spectroscopic (EIS) current changed and with increasing concentration of Trp, the peak current of Hem was linearly amplified (Fig. 3). The limit of detection of this biosensor for Trp was 0.026 nM (Hashkavayi and Raoof, 2017).

One of the effective electrochemical biosensors is based on DNA probes immobilized on electrode surface. E-DNA biosensors have full advantages such as independent probe configurational, high identification efficiencies, homogeneous electrochemical aptasensing strategies and protection of DNA under physiological conditions (Zhang et al., 2012a,b, 2016). Molecular imprinting polymers (MIPs) are one of the approaches for capturing the electroactive substances from solution on the electrode surface to increase response signals in homogeneous E-DNA biosensor (Yoshikawa et al., 2016). In this regard, You et al. designed biosensor based on gold nanoparticles-reduced graphene oxide (AuNPs-GO)-modified glass carbon electrode (GCE) which was coated with a specific MIPs for rhodamine B (RhB). The signal amplification section was SiO_2@Ag nanoparticles which was modified with DNA-probe (RhB-labled DNA) by Ag–S bond in order to form SiO_2@Ag/DNA complex for the detection of breast cancer susceptibility gene (BRCA-1). SiO_2@Ag acted as the signal amplifier and

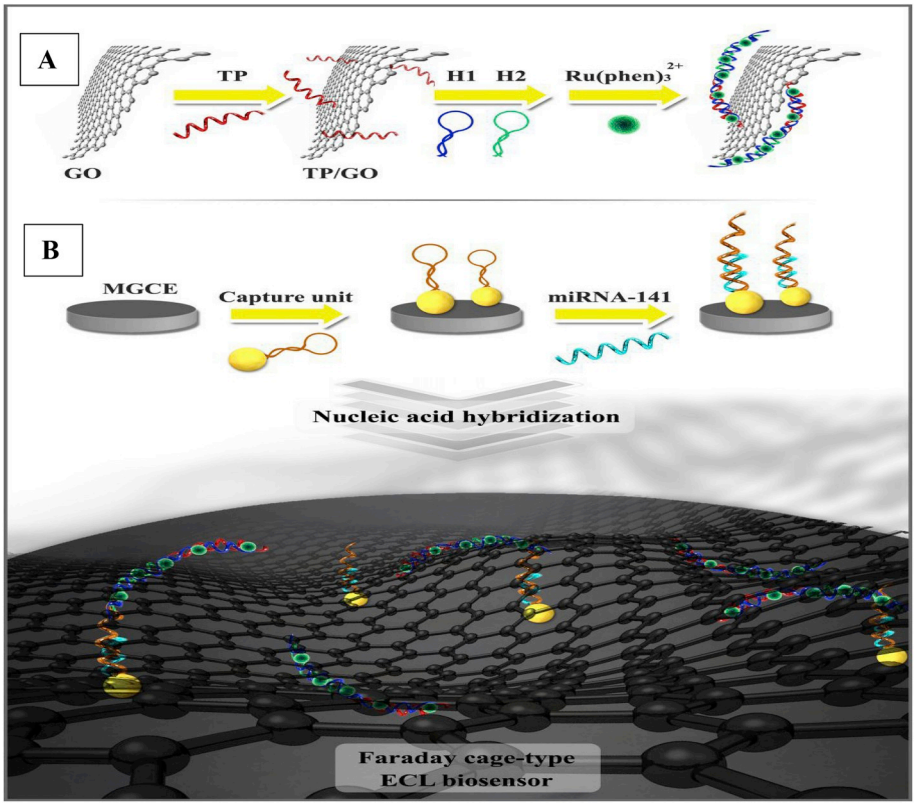

Fig. 2. Schematic diagram of (A) the preparation procedure of the signal unit (Ru $(phen)_3^{2+}$ HCR/GO) and (B) the fabrication of the proposed ECL biosensor for miRNA-141 detection. Reproduced with modification from (Lu et al., 2018a).

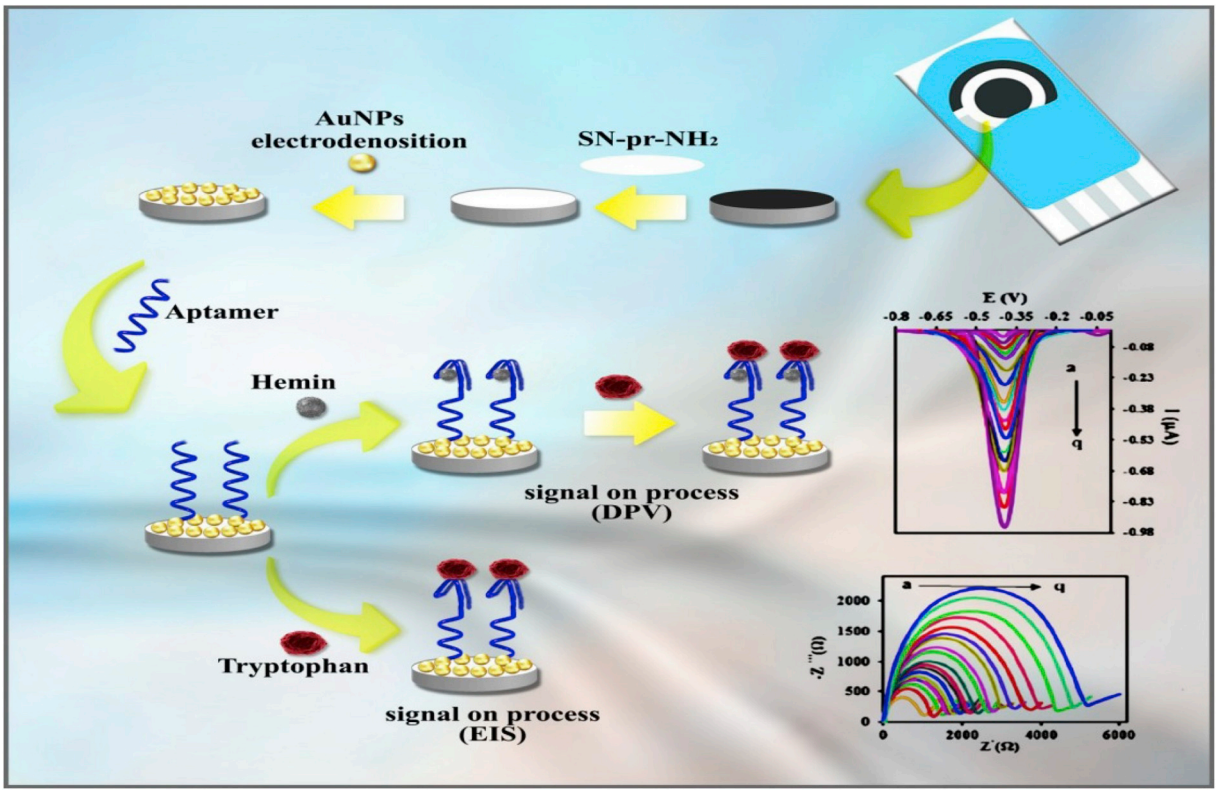

Fig. 3. Graphic illustration of the preparation of electrochemical aptasensor for Trp detection. Immobilization of aptamer for detection of tryptophan on the surface of the AuNPs/amine-functionalized silica nanoparticle was monitored by hemin (Hem) operating as electrochemical biosensor. Reproduced with modification from (Hashkavayi and Raoof, 2017).

electrochemical indicator.

In the presence of target, BRCA-1 DNA (target DNA) was hybridized with SiO_2@Ag-modified DNA and RhB-labeled DNA homogeneously and formed SiO_2@Ag/dsDNA/RhB complex (Fig. 4). The resultant complex was attached to the surface of MIPs-modified electrode which was recognized by RhB segment and produced electrochemical signals with a detection limit of 2.53 fM (You et al., 2018).

In another study, Cu/Ni/Ru and PEI@SiO_2 (SiO_2 as core and Au as shell) were applied as electrochemiluminescence (ECL) immunosensor for aflatoxins B1 (AFB1) detection. This ECL immunosensor is composed of two parts: (Cu/Ni/Ru) part acts as luminophor with high ECL efficiency while polyethylenimine-capped silicon dioxide (PEI@SiO_2) break the interaction between Ru and metal ions (Cu(II)/Ni(II)) thereby producing PEI and metal ions complex. Au–Cu/Ni/Ru could capture antibody-AFB1 and coalesce with antigen-AFB1. AuNPs on the PEI@-SiO_2 provided the required large surface area for interaction with AFB1-bovine serum albumin. Due to the formation of Au-PEI@SiO_2-AFB1-BSA structure, in the presence of free AFB1, the competitive binding occurred between free AFB1 and AFB1-BSA for interaction with antibody- AFB1 that was immobilized on Au–Cu/Ni/Ru leading to lower rate of formation of Au-PEI@SiO_2-AFB1-BSA–antibody complex. Due to the low interaction between Au-PEI@SiO_2-AFB1-BSA and antibodies, eventually, ECL signal was enhanced with augmenting the concentrations of the free AFB1 (Fig. 5). The limit of detection of this ultrasensitive immunosensor was about 0.0039 ng mL^{-1} (S/N = 3) (Wang et al., 2018).

In another study, Argoubi and coworkers designed an electrochemical aptasensor for PSA detection. The aptasensor was based on gold electrodes covered with aptamer-modified mesoporous silica thin films (MSF) (MSF on the surface of the Au electrode). The aptamer recognized the PSA with $[Fe(CN)_6]^{3/4-}$ redox diffusion aptitude of an electrochemical probe through the nanochannels of the mesoporous film gated by anti-PSA specific DNA aptamer with a limit of detection of 280 pg mL^{-1} (Argoubi et al., 2018).

High concentration of C-reactive protein (CRP) in serum would be attended as a primary indicator for infection and inflammation diseases such as cardiovascular disease (Bryan et al., 2013; Vashist et al., 2016). A large amount of zinc ions (Zn^{2+}) was immobilized on AuNPs-covered silica microspheres (immunoprobe) (mSiO_2 as core and AuNPs as shell) used as signal label in sensing field. These microspheres provided a large exterior region for immobilizing antibodies (Ab) and signal molecules (Zn^{2+}). Beside, RNA aptamers for CPR detection interact with AuNPs-coated electrode surface through gold-sulfur affinity. In the presence of CRP, aptamer-CRP-immunoprobe creates a sandwich structure. When a sandwich structure is formed, the electron transfer is blocked by RNA aptamer and CRP. Larger amount of zinc ions was immobilized on the surface area of AuNPs@SiMSs and the sensing signal clearly increased about −1.16 V. The limit of detection of this aptasensor was about 0.0017 ng mL^{-1} (Wang et al., 2017).

Other electrochemiluminescence sensors were presented in Table 4.

2.4. Colorimetric sensor

A colorimetric sensor is superior because the cost can be diminished and they can be made for portable real-time recognition. AuNPs with surface plasmon resonance (SPR) absorption properties provide strong vibrant color of their colloidal solutions. Hybrid of metallic nanocomposites are ideal attributes for the development of colorimetric sensors for target detection (Amendola et al., 2017). For example, covering the metallic nanocomposites with a thin layer of SiO_2 is a strategy to take advantage of SPR technology for monitoring the surface reactions. Detection limit of SPR biosensors are in the range of picomolar to femtomolar mass concentrations of analytes providing extremely high sensitivity (Law et al., 2011). It is reported that a powerful strategy for providing a wide optical bandwidth of AuNPs is to control the interparticle interactions of the silica-coated gold nanoparticles.

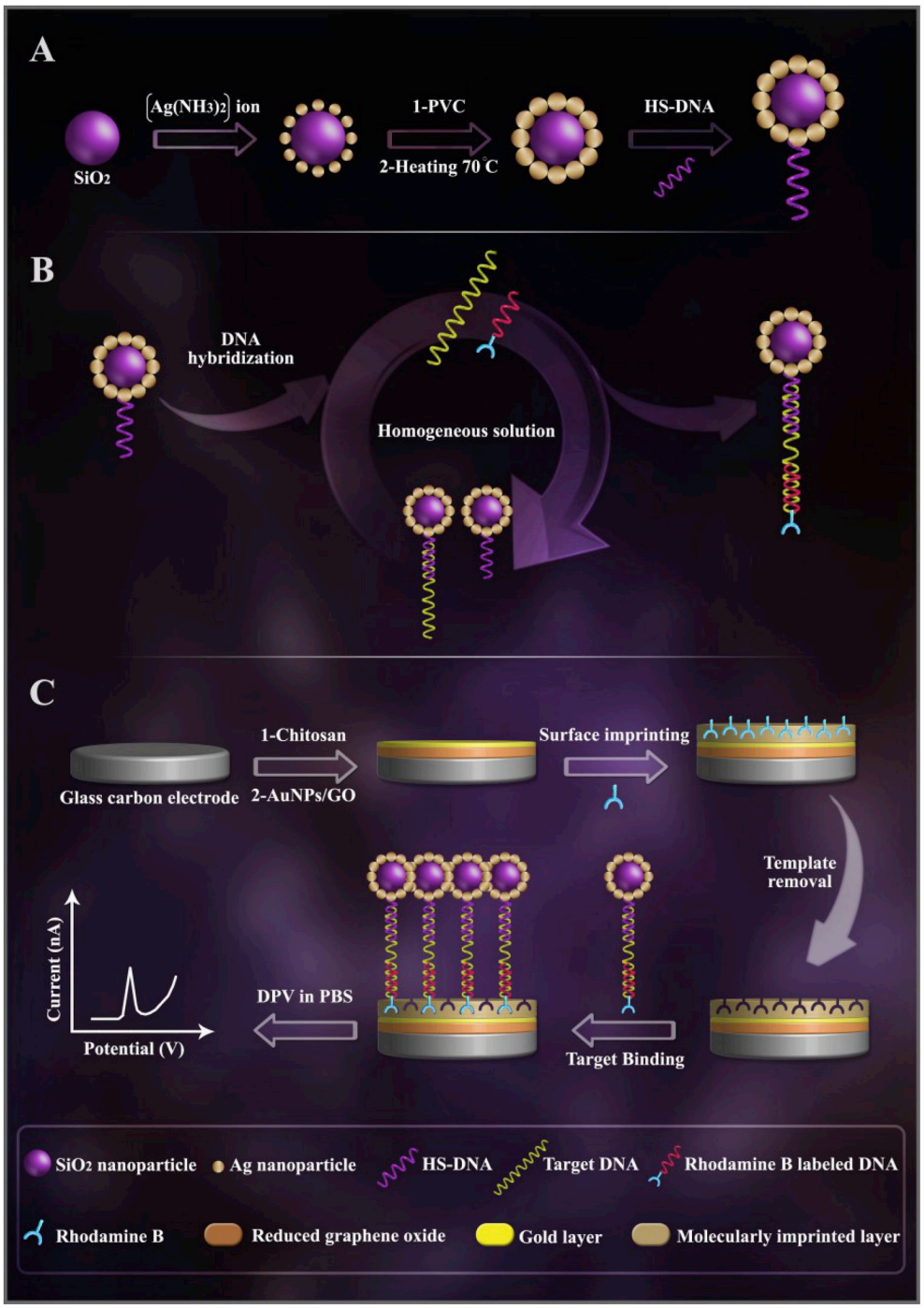

Fig. 4. Graphic illustration of the MIPs-based E-DNA biosensing. In panels (A) and (B), the target DNA homogeneously interacted with SiO_2@Ag-coated DNA and RhB-labeled DNA. (C), This nanocomposite was moved to the MIPs covered electrode surface thanks for imprinting cavities detection. Reproduced with modification from (You et al., 2018).

Since, diabetes is one of the most common diseases in the world; Luo et al. designed a colorimetric sensor to determine blood glucose concentrations for diabetic patients. The aforementioned sensor with fluorescence, superparamagnetism and peroxidase-like catalytic activity properties is consisted of Fe_3O_4@SiO_2@AuMNPs (Fe_3O_4 as core, SiO_2 as shell and AuNPs functionalized SiO_2) and was used to realize the concentration of H_2O_2 and glucose. Detection process of glucose with highly responsive, inexpensive and selective method was performed in two steps: The first step involved catalytic oxidation of glucose with glucose oxidase to produce H_2O_2 while in the second step, Fe_3O_4@SiO_2@AuMNPs catalyzed the oxidation reaction. Oxidation of 3,3′,5,5′-tetramethylbenzidine (TMB) by H_2O_2 generated TMBDI product with a change of color to blue. Eventually, Fe_3O_4@SiO_2@AuMNPs was separated by an external magnetic field. The limit of detection of this colorimetric sensor was 3 mM for glucose detection (Luo et al., 2017).

Considering that ascorbic acid (AA) as antioxidant plays an important role in the treatment and prevention of different diseases such as scurvy, cancer, kidney calculi, cardiovascular, precise determination of the amount of AA in the human body are essential. Gold nanorod@silver core–shell nanostructures coated with silica layer was applied for the detection of AA as colorimetric sensor. Mesoporous silica coating with elastic property affords a stable microenvironment around the

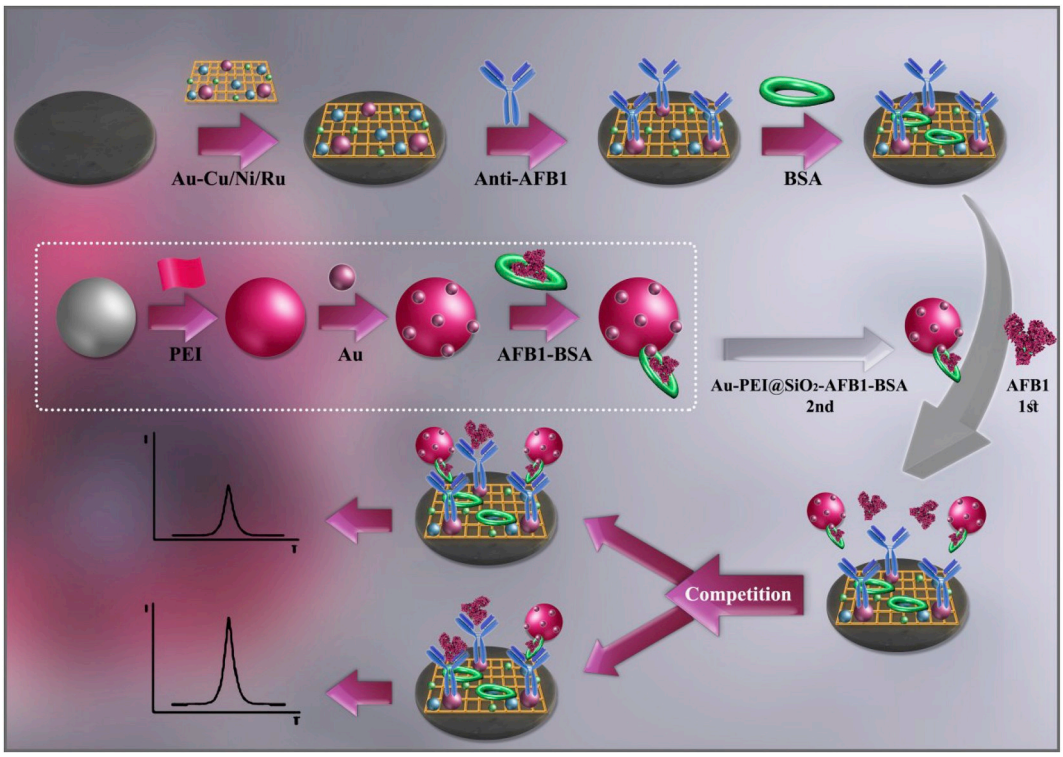

Fig. 5. Illustration of ECL immunosensor for AFB1 detection. This sensor is composed of two parts: (Cu/Ni/Ru) acts as luminophor with high ECL efficiency while polyethyleneimine capped silicon dioxide (PEI@SiO_2) break the interaction between Ru and metal ions (Cu(II)/Ni(II)) thereby producing PEI and metal ions complex. The luminophor part (Cu/Ni/Ru) interacts with antibody-AFB1. Then AuNPs on the surface of PEI@SiO_2 interacts with AFB1-bovine serum albumin and in the presence of free AFB1, competitive binding between free AFB1 and AFB1-BSA occurs. In this sensor, ECL signal is amplified with increasing the concentrations of the free AFB1. Reproduced with modification from (Wang et al., 2018). (For interpretation of the references to color in this figure legend, the reader is referred to the Web version of this article.)

Table 4
Representation of electrochemiluminescence (ECL) sensor based on silica-gold NPs.

Detection method	Nanoparticle	Detection Sample	LOD (CFU/ml)	Ref
Electrochemical sensor	PtAu supported on silica nanorods	H_2O_2	2.6 μM	Liu et al. (2018)
Electrochemical sensor	SiO_2@Au	Diuron	51.9 nmol/L	Sun et al. (2018a)
Electrochemical biosensor	SiO_2@$MoSe_2$ GO–AuNPs	DNA	0.068 fM	Shuai et al. (2017)
Electrochemiluminescence and immunosensor	GCE/tGO/Si-AuNPs	Cancer biomarkers (CEA and AFP)	–	Rashidiani et al. (2018)
Electrochemiluminescence sensor	Ru@SiO_2	fumonisin B1	0.35 pg mL^{-1}	Zhang et al. (2017)
Electrochemical sensor	GC/Au-MSM	Hydrazine (HZ) and nitrobenzene (NB)	0.11 μM and 15.0 nM	Gupta et al. (2017)
Electrochemical sensor	FS-Au-CA	17β-estradiol (EST)	0.0074 μM	Özcan and Topçuoğulları (2017)
Electrochemicalimunosensor	MSN-Th-Au	Prostate specific antigen (PSA)	0.31 pg mL^{-1}	Fan et al. (2016)
Electrochemical biosensor	MCM-41-Au	Caspase-3	5 fM	Khalilzadeh et al. (2016)
Electrochemiluminescence immunosensor	Ru–Si@Au	p53 protein	22.8 fM	Afsharan et al. (2016)
Electrochemical immunosensor	ATCP/SiO_2@Au/$p5315$ d- Ab,ATLP/SiO_2@Au/$p53392$ d-Ab	phosphor p^{5315} and phospho-p^{53392}	0.05 and 0.02 ng mL^{-1}	Ge et al. (2016)
Electrochemiluminescence sensor	Ru–SiO_2@PLL-Au	miRNA-21 and miRNA-141	6.3 and 8.6 fM	Feng et al. (2016)
Electrochemical sensor	GE-TDSN CGNP-PDDA	BSA	8.4×10^{-13} mol L^{-1}	Yari and Saeidikhah (2015)
Electrochemical sensor	GCE/Au-MSS	ascorbic acid and uric acid	1.65 μM and 2.14 μM	Gupta and Ganesan (2015)

AuNR@Ag nanostructure. Permanganate (MnO^{4-}) as a strong oxidizing agent played an important role in the sensing sensor. Silver shell was disappeared *via* the oxidation of silver atoms by MnO^{4-}. As a result of this reaction, a color and UV–Vis absorption change was observed. In the presence of AA molecules, the silver ions were reduced by the AA and the original morphology of the silver shell was formed on the surface of the AuNRs once again. This process led to change of localization of surface plasmon resonance (SPR) absorbance spectra. The SPR spectra band displayed an obvious blue shift when the concentration of AA was high. The detection limit of this admirable sensor was 0.03 mM (Chen et al., 2019).

3. Conclusion

The challenges including implementation of non-biocompatible chemicals in sensor platform, expensive instrumentation, label free and low detection limit, real time sample analysis and easily handling detection procedure constitute limiting factors for the conventional

sensors available in the market.

The implementation of nanotechnology for fabrication of sensory systems is the ultimate goal in the sensing technology for rapid, sensitive and low cost detection.

Hybridization is an interesting approach in which combined components provide the opportunity to modify their individual characteristics. Hybridization technique simultaneously poses challenges and opportunities. The crucial concern is the ability of synthesized hybrid materials to enhance the ideal characteristics of each component while decreasing their shortcomings. Addressing the aforementioned concern may lead to a desirable strategy for the development of novel materials with synergic properties and new characteristics leading to improved performance of the current sensory systems.

Another obstacle in these technologies is sample preparation. Sensors implementing hybrid silica-golds materials depending on analyte nature could induce differences in electrical, optical, or mechanical characteristics of the sensors. It should be noted that real samples usually contain many components that could interfere with ligand-target association, and in turn, such alterations decrease the sensor sensitivity. Therefore, the downstream procedures for analytes detection are crucial for achieving desirable detection limit.

Silica-gold hybrid platforms greatly extend the range of materials available to sensing technology. Silica can offer opportunities to modify its mechanical characteristics, thereby facilitating the production of films, fibers, nanosheets, spheres, foam and core shells to attain various inorganic structures for providing desirable optical, porosity and hydrophilic/hydrophobic balance of the platform. Moreover, Silica nanomaterials can change the optical properties of gold nanomaterials when they combined to form a hybrid entity. The shape, size and structure of both silica and gold could influence the properties of the fabricated hybrids.

AuNPs in the silica-gold hybrid systems exhibit specific electrical and optical properties, thus providing unique electrochemical, chemical or biochemical performance.

In this regard, the use of gold-silica hybrid materials might lead to further advances in the development of highly sensitive and specific assays for analytes detection.

Declaration of competing interest

The authors declare that they have no known competing financial interests or personal relationships that could have appeared to influence the work reported in this paper.

CRediT authorship contribution statement

Elnaz Bagheri: Writing - original draft. **Legha Ansari:** Writing - original draft. **Elham Sameiyan:** Writing - original draft. **Khalil Abnous:** Writing - original draft. **Seyed Mohammad Taghdisi:** Writing - original draft. **Mohammad Ramezani:** Conceptualization, Writing - review & editing. **Mona Alibolandi:** Conceptualization, Writing - review & editing.

Acknowledgements

The authors are grateful to Mashhad University of Medical Sciences for its financial support.

References

Afsharan, H., Navaeipour, F., Khalilzadeh, B., Tajalli, H., Mollabashi, M., Ahar, M.J., Rashidi, M.-R., 2016. Highly sensitive electrochemiluminescence detection of p53 protein using functionalized Ru–silica nanoporous@ gold nanocomposite. Biosens. Bioelectron. 80, 146–153.

Amendola, V., Pilot, R., Frasconi, M., Marago, O.M., Iati, M.A., 2017. Surface plasmon resonance in gold nanoparticles: a review. J. Phys. Condens. Matter 29 (20), 203002.

Argoubi, W., Sánchez, A., Parrado, C., Raouafi, N., Villalonga, R., 2018. Label-free electrochemical aptasensing platform based on mesoporous silica thin film for the detection of prostate specific antigen. Sensor. Actuator. B Chem. 255, 309–315.

Bagheri, E., Abnous, K., Alibolandi, M., Ramezani, M., Taghdisi, S.M., 2018. Triple-helix molecular switch-based aptasensors and DNA sensors. Biosens. Bioelectron. 111, 1–9.

Bracamonte, M.V., Melchionna, M., Giuliani, A., Nasi, L., Tavagnacco, C., Prato, M., Fornasiero, P., 2017. H2O2 sensing enhancement by mutual integration of single walled carbon nanohorns with metal oxide catalysts: the CeO2 case. Sensor. Actuator. B Chem. 239, 923–932.

Bryan, T., Luo, X., Bueno, P.R., Davis, J.J., 2013. An optimised electrochemical biosensor for the label-free detection of C-reactive protein in blood. Biosens. Bioelectron. 39 (1), 94–98.

Capuron, L., Ravaud, A., Neveu, P., Miller, A., Maes, M., Dantzer, R., 2002. Association between decreased serum tryptophan concentrations and depressive symptoms in cancer patients undergoing cytokine therapy. Mol. Psychiatr. 7 (5), 468.

Chakraborty, I., Mascharak, P.K., 2016. Mesoporous silica materials and nanoparticles as carriers for controlled and site-specific delivery of gaseous signaling molecules. Microporous Mesoporous Mater. 234, 409–419.

Chand, R., Neethirajan, S., 2017. Microfluidic platform integrated with graphene-gold nano-composite aptasensor for one-step detection of norovirus. Biosens. Bioelectron. 98, 47–53.

Chen, L., Lin, M., Yang, P., 2019. Reproducible mesoporous silica-coated gold@silver nanoprobes for the bright colorimetric sensing of ascorbic acid. New J. Chem. 43, 10841–10849.

Chen, M., Luo, W., Zhang, Z., Zhu, F., Liao, S., Yang, H., Chen, X., 2017. Sensitive surface enhanced Raman spectroscopy (SERS) detection of methotrexate by core-shell-satellite magnetic microspheres. Talanta 171, 152–158.

Cissell, K.A., Shrestha, S., Deo, S.K., 2007. MicroRNA Detection: Challenges for the Analytical Chemist. ACS Publications.

Clarkson, T.W., Magos, L., Myers, G.J., 2003. The toxicology of mercury—current exposures and clinical manifestations. N. Engl. J. Med. 349 (18), 1731–1737.

Dhara, S., Chandra, S., Magudapathy, P., Kalavathi, S., Panigrahi, B., Nair, K., Sastry, V., Hsu, C., Wu, C., Chen, K., 2004. Blue luminescence of Au nanoclusters embedded in silica matrix. J. Chem. Phys. 121 (24), 12595–12599.

Du, F.-K., Zhang, H., Tan, X.-C., Yan, J., Liu, M., Chen, X., Wu, Y.-Y., Feng, D.-F., Chen, Q.-Y., Cen, J.-M., 2018. Ru (bpy) 32+-Silica@ Poly-L-lysine-Au as labels for electrochemiluminescence lysozyme aptasensor based on 3D graphene. Biosens. Bioelectron. 106, 50–56.

Emrani, A.S., Danesh, N.M., Ramezani, M., Taghdisi, S.M., Abnous, K., 2016. A novel fluorescent aptasensor based on hairpin structure of complementary strand of aptamer and nanoparticles as a signal amplification approach for ultrasensitive detection of cocaine. Biosens. Bioelectron. 79, 288–293.

Fan, D., Li, N., Ma, H., Li, Y., Hu, L., Du, B., Wei, Q., 2016. Electrochemical immunosensor for detection of prostate specific antigen based on an acid cleavable linker into MSN-based controlled release system. Biosens. Bioelectron. 85, 580–586.

Feng, X., Gan, N., Zhang, H., Li, T., Cao, Y., Hu, F., Jiang, Q., 2016. Ratiometric biosensor array for multiplexed detection of microRNAs based on electrochemiluminescence coupled with cyclic voltammetry. Biosens. Bioelectron. 75, 308–314.

Fuerea, A., Baciarello, G., Patrikidou, A., Albigès, L., Massard, C., Di Palma, M., Escudier, B., Fizazi, K., Loriot, Y., 2016. Early PSA response is an independent prognostic factor in patients with metastatic castration-resistant prostate cancer treated with next-generation androgen pathway inhibitors. Eur. J. Canc. 61, 44–51.

Gaylord, B.S., Massie, M.R., Feinstein, S.C., Bazan, G.C., 2005. SNP detection using peptide nucleic acid probes and conjugated polymers: applications in neurodegenerative disease identification. Proc. Natl. Acad. Sci. Unit. States Am. 102 (1), 34–39.

Ge, X., Zhang, A., Lin, Y., Du, D., 2016. Simultaneous immunoassay of phosphorylated proteins based on apoferritin templated metallic phosphates as voltammetrically distinguishable signal reporters. Biosens. Bioelectron. 80, 201–207.

Gupta, R., Ganesan, V., 2015. Gold nanoparticles impregnated mesoporous silica spheres for simultaneous and selective determination of uric acid and ascorbic acid. Sensor. Actuator. B Chem. 219, 139–145.

Gupta, R., Rastogi, P.K., Ganesan, V., Yadav, D.K., Sonkar, P.K., 2017. Gold nanoparticles decorated mesoporous silica microspheres: a proficient electrochemical sensing scaffold for hydrazine and nitrobenzene. Sensor. Actuator. B Chem. 239, 970–978.

Hashkavayi, A.B., Raoof, J.B., 2017. Design an aptasensor based on structure-switching aptamer on dendritic gold nanostructures/Fe3O4@ SiO2/DABCO modified screen printed electrode for highly selective detection of epirubicin. Biosens. Bioelectron. 91, 650–657.

Ji, S., Guo, Q., Yue, Q., Wang, L., Wang, H., Zhao, J., Dong, R., Liu, J., Jia, J., 2011. Controlled synthesis of Pt nanoparticles array through electroreduction of cisplatin bound at nucleobases terminated surface and application into H2O2 sensing. Biosens. Bioelectron. 26 (5), 2067–2073.

Khalilzadeh, B., Charoudeh, H.N., Shadjou, N., Mohammad-Rezaei, R., Omidi, Y., Velaei, K., Aliyari, Z., Rashidi, M.-R., 2016. Ultrasensitive caspase-3 activity detection using an electrochemical biosensor engineered by gold nanoparticle functionalized MCM-41: its application during stem cell differentiation. Sensor. Actuator. B Chem. 231, 561–575.

Knott, P., Curzon, G., 1972. Free tryptophan in plasma and brain tryptophan metabolism. Nature 239 (5373), 452.

Ko, J., Lee, C., Choo, J., 2015. Highly sensitive SERS-based immunoassay of aflatoxin B1 using silica-encapsulated hollow gold nanoparticles. J. Hazard Mater. 285, 11–17.

Lavenn, C., Albrieux, F., Bergeret, G., Chiriac, R., Delichere, P., Tuel, A., Demessence, A., 2012. Functionalized gold magic clusters: Au 25 (SPhNH 2) 17. Nanoscale 4 (23), 7334–7337.

Lavenn, C., Demessence, A., Tuel, A., 2014. Atomically well-defined Au25 (SR) 17/18 nanoclusters deposited on silica supports for the aerobic epoxidation of trans-stilbene. Catal. Today 235, 72–78.
Law, W.-C., Yong, K.-T., Baev, A., Prasad, P.N., 2011. Sensitivity improved surface plasmon resonance biosensor for cancer biomarker detection based on plasmonic enhancement. ACS Nano 5 (6), 4858–4864.
Li, P., Ma, B., Yang, L., Liu, J., 2015a. Hybrid single nanoreactor for in situ SERS monitoring of plasmon-driven and small Au nanoparticles catalyzed reactions. Chem. Commun. 51 (57), 11394–11397.
Li, X., Wang, Y., Luo, J., Ai, S., 2016. Sensitive detection of adenosine triphosphate by exonuclease III-assisted cyclic amplification coupled with surface plasmon resonance enhanced fluorescence based on nanopore. Sensor. Actuator. B Chem. 228, 509–514.
Li, Z., Wang, Y., Ni, Y., Kokot, S., 2015b. Fluorescence analysis of 6-mercaptopurine with the use of a nano-composite consisting of BSA-capped Au nano-clusters and core–shell Fe3O4–SiO2 nanoparticles. Biosens. Bioelectron. 70, 246–253.
Liu, B., Han, G., Zhang, Z., Liu, R., Jiang, C., Wang, S., Han, M.-Y., 2011. Shell thickness-dependent Raman enhancement for rapid identification and detection of pesticide residues at fruit peels. Anal. Chem. 84 (1), 255–261.
Liu, M., He, S., Chen, W., 2014. Co 3 O 4 nanowires supported on 3D N-doped carbon foam as an electrochemical sensing platform for efficient H 2 O 2 detection. Nanoscale 6 (20), 11769–11776.
Liu, S., Cheng, C., Liu, T., Wang, L., Gong, H., Li, F., 2015. Highly sensitive fluorescence detection of target DNA by coupling exonuclease-assisted cascade target recycling and DNAzyme amplification. Biosens. Bioelectron. 63, 99–104.
Liu, W., Hiekel, K., Hübner, R., Sun, H., Ferancova, A., Sillanpää, M., 2018. Pt and Au bimetallic and monometallic nanostructured amperometric sensors for direct detection of hydrogen peroxide: influences of bimetallic effect and silica support. Sensor. Actuator. B Chem. 255, 1325–1334.
Lu, J., Wu, L., Hu, Y., Wang, S., Guo, Z., 2018a. Ultrasensitive Faraday cage-type electrochemiluminescence assay for femtomolar miRNA-141 via graphene oxide and hybridization chain reaction-assisted cascade amplification. Biosens. Bioelectron. 109, 13–19.
Lu, Y., Zhong, J., Yao, G., Huang, Q., 2018b. A label-free SERS approach to quantitative and selective detection of mercury (II) based on DNA aptamer-modified SiO2@ Au core/shell nanoparticles. Sensor. Actuator. B Chem. 258, 365–372.
Luo, S., Liu, Y., Rao, H., Wang, Y., Wang, X., 2017. Fluorescence and magnetic nanocomposite Fe3O4@ SiO2@ Au MNPs as peroxidase mimetics for glucose detection. Anal. Biochem. 538, 26–33.
Manso, S., Pezo, D., Gómez-Lus, R., Nerín, C., 2014. Diminution of aflatoxin B1 production caused by an active packaging containing cinnamon essential oil. Food Contr. 45, 101–108.
Moreira, A.F., Dias, D.R., Correia, I.J., 2016. Stimuli-responsive mesoporous silica nanoparticles for cancer therapy: a review. Microporous Mesoporous Mater. 236, 141–157.
Niu, C., Song, Q., He, G., Na, N., Ouyang, J., 2016. Near-infrared-fluorescent probes for bioapplications based on silica-coated gold nanobipyramids with distance-dependent plasmon-enhanced fluorescence. Anal. Chem. 88 (22), 11062–11069.
Özcan, A., Topçuoğulları, D., 2017. Voltammetric determination of 17-β-estradiol by cysteamine self-assembled gold nanoparticle modified fumed silica decorated graphene nanoribbon nanocomposite. Sensor. Actuator. B Chem. 250, 85–90.
Phatangare, A., Dhole, S., Dahiwale, S., Bhoraskar, V., 2018. Ultra-high sensitive substrates for surface enhanced Raman scattering, made of 3 nm gold nanoparticles embedded on SiO2 nanospheres. Appl. Surf. Sci. 441, 744–753.
Rashidiani, J., Kamali, M., Sedighian, H., Akbariqomi, M., Mansouri, M., Kooshki, H., 2018. Ultrahigh sensitive enhanced-electrochemiluminescence detection of cancer biomarkers using silica NPs/graphene oxide: a comparative study. Biosens. Bioelectron. 102, 226–233.
Sápi, A., Dobó, D.G., Sebők, D.n., Halasi, G., Juhász, K.L., Szamosvölgyi, A.k., Pusztai, P., Varga, E., Kálomista, I., Galbács, G., 2017. Silica-based catalyst supports are inert, are they not?: striking differences in ethanol decomposition reaction originated from meso-and surface-fine-structure evidenced by small-angle X-ray scattering. J. Phys. Chem. C 121 (9), 5130–5136.
Shim, J., Lee, J., Ye, Y., Hwang, J., Kim, S.-K., Lim, T.-H., Wiesner, U., Lee, J., 2012. One-pot synthesis of intermetallic electrocatalysts in ordered, large-pore mesoporous carbon/silica toward formic acid oxidation. ACS Nano 6 (8), 6870–6881.
Shuai, H.-L., Wu, X., Huang, K.-J., Zhai, Z.-B., 2017. Ultrasensitive electrochemical biosensing platform based on spherical silicon dioxide/molybdenum selenide nanohybrids and triggered hybridization chain reaction. Biosens. Bioelectron. 94, 616–625.
Smith, L., Mohr, L., Raftery, M., 1973. Mechanism for lysozyme-catalyzed hydrolysis. J. Am. Chem. Soc. 95 (22), 7497–7500.
Song, Y., Li, Y., Xu, Q., Liu, Z., 2017. Mesoporous silica nanoparticles for stimuli-responsive controlled drug delivery: advances, challenges, and outlook. Int. J. Nanomed. 12, 87.
Sousa-Castillo, A., Gauthier, M., Arenal, R., Pérez-Lorenzo, M., Correa-Duarte, M.A., 2015. Engineering microencapsulation of highly catalytic gold nanoclusters for an extreme thermal stability. Nanoscale 7 (48), 20584–20592.
Sun, J., Gan, T., Zhai, R., Fu, W., Zhang, M., 2018a. Sensitive and selective electrochemical sensor of diuron against indole-3-acetic acid based on core-shell structured SiO 2@ Au particles. Ionics 24 (8), 2465–2472.
Sun, M., Zhao, A., Wang, D., Wang, J., Chen, P., Sun, H., 2018b. Cube-like Fe3O4@ SiO2@ Au@ Ag magnetic nanoparticles: a highly efficient SERS substrate for pesticide detection. Nanotechnology 29 (16), 165302.
Taei, M., Hadadzadeh, H., Hasanpour, F., Tavakkoli, N., Dolatabadi, M.H., 2015. Simultaneous electrochemical determination of ascorbic acid, epinephrine, and uric acid using a polymer film-modified electrode based on Au nanoparticles/poly (3, 3′, 5, 5′-tetrabromo-m-cresolsulfonphthalein). Ionics 21 (12), 3267–3278.
Thatai, S., Khurana, P., Prasad, S., Kumar, D., 2015. Plasmonic detection of Cd2+ ions using surface-enhanced Raman scattering active core–shell nanocomposite. Talanta 134, 568–575.
Vashist, S.K., Venkatesh, A., Schneider, E.M., Beaudoin, C., Luppa, P.B., Luong, J.H., 2016. Bioanalytical advances in assays for C-reactive protein. Biotechnol. Adv. 34 (3), 272–290.
Wang, C., Chen, L., Qi, Z., 2013a. One-pot synthesis of gold nanoparticles embedded in silica for cyclohexane oxidation. Catal. Sci. Technol. 3 (4), 1123–1128.
Wang, H., Xu, C., Zheng, C., Xu, W., Dong, T., Liu, K., Han, H., Liang, J., 2013b. Facile synthesis and characterization of Au nanoclusters-silica fluorescent composite nanospheres. J. Nanomater. 22, 2013.
Wang, J., Guo, J., Zhang, J., Zhang, W., Zhang, Y., 2017. RNA aptamer-based electrochemical aptasensor for C-reactive protein detection using functionalized silica microspheres as immunoprobes. Biosens. Bioelectron. 95, 100–105.
Wang, Y., Zhao, G., Li, X., Liu, L., Cao, W., Wei, Q., 2018. Electrochemiluminescent competitive immunosensor based on polyethyleneimine capped SiO2 nanomaterials as labels to release Ru (bpy) 32+ fixed in 3D Cu/Ni oxalate for the detection of aflatoxin B1. Biosens. Bioelectron. 101, 290–296.
Wang, Z., Liu, N., Feng, F., Ma, Z., 2015. Synthesis of cadmium, lead and copper alginate nanobeads as immunosensing probes for the detection of AFP, CEA and PSA. Biosens. Bioelectron. 70, 98–105.
Ya, Y., Luo, D., Zhan, G., Li, C., 2008. Electrochemical investigation of tryptophan at a poly (p-aminobenzene sulfonic acid) film modified glassy carbon electrode. Bull. Kor. Chem. Soc. 29 (5), 928.
Yang, L., Li, N., Wang, K., Hai, X., Liu, J., Dang, F., 2018. A novel peptide/Fe3O4@ SiO2-Au nanocomposite-based fluorescence biosensor for the highly selective and sensitive detection of prostate-specific antigen. Talanta 179, 531–537.
Yari, A., Saeidikhah, M., 2015. Ultra-trace electrochemical impedance determination of bovine serum albumin by a two dimensional silica network citrate-capped gold nanoparticles modified gold electrode. Talanta 144, 1336–1341.
Yoshikawa, M., Tharpa, K., Dima, S.-O., 2016. Molecularly imprinted membranes: past, present, and future. Chem. Rev. 116 (19), 11500–11528.
You, M., Yang, Sh, Tang, W., Zhang, F., He, P., 2018. Molecularly imprinted polymers-based electrochemical DNA biosensor for the determination of BRCA-1 amplified by SiO2@Ag. Biosens. Bioelectron. 112, 72–78.
Zhang, F.-T., Cai, L.-Y., Zhou, Y.-L., Zhang, X.-X., 2016. Immobilization-free DNA-based homogeneous electrochemical biosensors. Trac. Trends Anal. Chem. 85, 17–32.
Zhang, H., Fu, C., Yi, Y., Zhou, X., Zhou, C., Ying, G., Shen, Y., Zhu, Y., 2018. A magnetic-based SERS approach for highly sensitive and reproducible detection of cancer-related serum microRNAs. Anal. Methods 10 (6), 624–633.
Zhang, H., Li, F., Dever, B., Li, X.-F., Le, X.C., 2012a. DNA-mediated homogeneous binding assays for nucleic acids and proteins. Chem. Rev. 113 (4), 2812–2841.
Zhang, J., Zhou, Ch, You, M., Liu, J., 2012b. Different sized luminescent gold nanoparticles. Nanoscale 4 (14), 4073–4083.
Zhang, W., Xiong, H., Chen, M., Zhang, X., Wang, S., 2017. Surface-enhanced molecularly imprinted electrochemiluminescence sensor based on Ru@ SiO2 for ultrasensitive detection of fumonisin B1. Biosens. Bioelectron. 96, 55–61.
Zhou, Z., Peng, S., Sui, M., Chen, S., Huang, L., Xu, H., Jiang, T., 2018. Multifunctional nanocomplex for surface-enhanced Raman scattering imaging and near-infrared photodynamic antimicrobial therapy of vancomycin-resistant bacteria. Colloids Surf. B Biointerfaces 161, 394–402.
Zhu, T., Hu, Y., Yang, K., Dong, N., Yu, M., Jiang, N., 2018. A novel SERS nanoprobe based on the use of core-shell nanoparticles with embedded reporter molecule to detect E. coli O157: H7 with high sensitivity. Microchim. Acta 185 (1), 30.
Zhu, W., Xuan, C., Liu, G., Chen, Z., Wang, W., 2015. A label-free fluorescent biosensor for determination of bovine serum albumin and calf thymus DNA based on gold nanorods coated with acridine orange-loaded mesoporous silica. Sensor. Actuator. B Chem. 220, 302–308.
Zou, Y., Yang, F., Yuan, X., Ma, K., Li, H., Zhao, X., Cai, N., Huang, X., Liu, W., 2017. An efficient sodium citrate-promoted synthetic method for the preparation of AuNPs@ mesoSiO2 for surface enhanced Raman spectroscopy in the detection of diluted blood. J. Saudi Chem. Soc. 21 (8), 1007–1012.